Journal of Sound and Vibration (1982) **84**(2), 173–189

THE DYNAMICS OF REPEATED IMPACTS WITH A SINUSOIDALLY VIBRATING TABLE

P. J. HOLMES†

Department of Theoretical and Applied Mechanics and Center for Applied Mathematics, Cornell University, Ithaca, New York 14853, *U.S.A.*

(*Received* 28 *October* 1981)

A deceptively simple difference equation is derived which approximately describes the motion of a small ball bouncing vertically on a massive sinusoidally vibrating plate. In the case of perfect elastic impacts, the equation reduces to the "standard mapping" which has been extensively studied by physicists in connection with the motions of particles constrained in potential wells. It is shown that, for sufficiently large excitation velocities and a coefficient of restitution close to one, this deterministic dynamical system exhibits large families of irregular non-periodic solutions in addition to the expected harmonic and subharmonic motions. The physical significance of these and other chaotic motions which appear to occur frequently in non-linear oscillations is discussed.

1. INTRODUCTION

Recently Wood and Byrne [1] studied a simple model impact process relevant to the study of noise generation in machinery. In their model, a small ball bounces vertically on a massive vibrating table, each impact being governed by the relationship

$$V(t_j) - W(t_j) = -\alpha(U(t_j) - W(t_j)), \tag{1}$$

where U, V and W are, respectively, the absolute velocities of the approaching ball, the departing ball and the table, $0 < \alpha \leqslant 1$ is the coefficient of restitution and $t = t_j$ is the time of the jth impact. It is assumed that the impact does not affect the velocity of the table. All velocities in equation (1) are measured vertically upward and it is assumed that the ball reverses its direction in the impact, which it will if $|U(t_j)| \gg |W(t_j)|$ ($W(t_j)$ must be greater than $U(t_j)$ for impact to occur at all). If one further assumes that the distance the ball travels between impacts under the influence of the gravitational acceleration, g, is large compared with the overall displacement of the table, then the time interval between impacts is easily approximated as

$$t_{j+1} - t_j = 2V(t_j)/g, \tag{2}$$

and the velocity of approach at the $(j+1)$st impact as

$$U(t_{j+1}) = -V(t_j). \tag{3}$$

Combining equations (1), (2) and (3) gives the recurrence relationship relating the state of the system at the $(j+1)$st impact to that at the jth in the form of a non-linear mapping, or pair of difference equations:

$$t_{j+1} = t_j + 2V_j/g, \qquad V_{j+1} = \alpha V_j + (1+\alpha)W(t_j + 2V_j/g), \tag{4}$$

† Work supported by NSF grant MEA 80-17570 and ARO contract DAAG-29C-0086.

0022-460X/82/180173 + 17 $03.00/0

where $V_j = V(t_j)$. Since the ball is in free flight between impacts, the dynamics is completely determined by V_j and t_j, which one can therefore call the *state* of the system at the jth step.

Wood and Byrne [1] studied the behavior of such a system for the case of random (Gaussian) excitation W. In their paper they mentioned experimental evidence which suggests that, even with sinusoidal excitation, apparently random, non-periodic motions are observed, if the excitation level is sufficiently high. In this paper it is proved that such motions do indeed occur in the deceptively simple mapping (4), and a topological description of (some of) them is given.

It is convenient to non-dimensionalize equations (4). With the displacement of the plate expressed as $-\beta \sin \omega t$, then $W = -\omega\beta \cos \omega t$ (the negative sign is chosen for convenience in subsequent calculations). In terms of the non-dimensional time $\phi = \omega t$ and velocity $v = 2\omega V/g$, and with $\gamma = 2\omega^2(1+\alpha)\beta/g$, one obtains the mapping $f = f_{\alpha,\gamma}$:

$$f: \qquad \phi_{j+1} = \phi_j + V_j, \qquad V_{j+1} = \alpha V_j - \gamma \cos(\phi_j + V_j). \tag{5}$$

In the mapping (5) γ plays the role of force amplitude and α of dissipation. It is easy to verify that the mapping (5) is a smooth invertible one, or diffeomorphism [2], its inverse being given by

$$f^{-1}: \qquad \phi_{j-1} = \phi_j - (1/\alpha)(\gamma \cos \phi_j + V_j), \qquad v_{j-1} = (1/\alpha)(\gamma \cos \phi_j + V_j). \tag{6}$$

Note that for $\alpha = 1$ (perfect elastic impacts) the mapping is area preserving, since then the determinant of the Jacobian

$$\det(Df) = \det \begin{bmatrix} 1 & 1 \\ \gamma \sin(\phi_j + V_j) & \alpha + \gamma \sin(\phi_j + V_j) \end{bmatrix} = \alpha \tag{7}$$

is unity. Also the mapping is invariant under the translation $\phi \mapsto \phi + 2n\pi$, and hence is 2π-periodic in ϕ, so that the (ϕ, v) state space is topologically the cylinder, $S^1 \times \mathbb{R}$, rather than the plane. This is important in the subsequent analysis.

The area preserving case, $\alpha = 1$, has been intensively studied, mostly by physicists (on account of its relevance to certain problems in particle physics), including Taylor [3], Chirikov [4], Greene [5] and Lichtenberg, Lieberman and Cohen [6], for example. In their work a slightly different co-ordinate system is chosen and the diffeomorphism is referred to as "the standard map". Moreover, Pustylnikov [7–9] considered the mechanical problem outlined above and derived an exact mapping for the case of general periodic excitation and showed that both it and the approximate mapping (5) have open sets of initial conditions (ϕ_0, v_0) such that $v_n \to \infty$ as $n \to \infty$ for suitable finite values of γ and $\alpha = 1$. Along with these unbounded motions, sets of bounded periodic motions are also found and numerical computations suggest that bounded non-periodic motions also exist (cf. references [4, 5]).

In references [4] and [5] the "transition to stochasticity", which occurs as γ is increased, is considered. For small γ all orbits remain bounded and most of them behave in a regular (=periodic or quasiperiodic) manner, but as γ increases the initially small regions filled with chaotic or stochastic motions grow until the phase space is ultimately almost completely filled with non-periodic motions. Various heuristic criteria, involving a delicate analysis of the stabilities of long period motions, have been derived to aid in the analysis of this transition. The interested reader is referred to Green's excellent survey [5] or the provocative paper of Chirikov [4] for more information. For general background on "stochastic" Hamiltonian systems see the monograph of Lichtenberg and Lieberman [10].

This paper is concerned with the effects of dissipation ($\alpha \neq 1$). Chirikov and Izraelev [11] considered a different dissipative modification of the standard map but otherwise

little work has been done in this area. Initially one might think that all complex behavior mentioned above would disappear with the addition of damping. However in other oscillatory problems in which periodic forcing and damping are applied it is known that sustained chaotic motions are observed [12–15]. Precisely the same phenomenon occurs in the mapping (5), and this is proved in section 3. Before this, in section 2 a brief review is provided of some aspects of two dimensional mappings and some of the simple periodic motions exhibited by the mapping (5) and their realizations in the motions of the bouncing ball are discussed. In sections 3–5, a global analysis of the map is presented and in sections 4 and 5 some aspects of the complicated invariant sets and bifurcations which occur as γ is increased for fixed $\alpha < 1$ are discussed. Finally, in section 6 some physical conclusions are drawn and mention is made of some other, similar, impact governed problems.

2. FIXED POINTS, PERIODIC ORBITS AND LOCAL BIFURCATIONS

Before considering periodic behavior in particular, it is helpful to recognize that there is one major difference between the dissipation free and dissipative cases. As already noted, Pustylnikov [9] showed that the mapping (5) with $\alpha = 1$ possesses unbounded orbits for suitable (large) values of γ. It is easy to see that no such orbits exist for $\alpha < 1$, provided that γ is bounded, since, from equations (5),

$$|v_{i+1}| \leq |\alpha v_i - \gamma \cos(\phi_i + v_i)| \leq \alpha |v_i| + \gamma. \tag{8}$$

(Recall that, while it has been assumed that $v > 0$ for physical reasons, the mapping is well defined for all $-\infty < v < \infty$.) Thus, if

$$|v_i| > \gamma/(1-\alpha), \tag{9}$$

one finds that $|v_{i+1}| < |v_i|$, implying that all orbits remain bounded and, in fact, must enter a strip bounded by $v = \pm\gamma/(1-\alpha)$ as j increases.

One can now seek fixed points of the mapping f: points $(\bar{\phi}, \bar{v})$ such that $f(\bar{\phi}, \bar{v}) = (\bar{\phi}, \bar{v})$. From equations (5) these are easily found to occur in pairs:

$$(\bar{\phi}_n, \bar{v}_n) = (\arccos(2n\pi(\alpha-1)/\gamma), 2n\pi), \qquad n = 0, \pm 1, \pm 2, \ldots, \pm N, \tag{10}$$

where N is the greatest integer such that

$$2N\pi(1-\alpha) < \gamma. \tag{11}$$

In deriving equation (10) use has been made of the periodicity of the state space, by setting

$$\phi = \phi + 2n\pi, \qquad n = 0, \pm 1, \pm 2, \ldots. \tag{12}$$

The stability of these fixed points is determined by the linearized map, Df, of equation (7). For a good review of such matters, with mechanical applications in mind, see reference [16], or [17]. If both eigenvalues are inside the unit circle in the complex plane ($|\lambda_i| < 1$), one has a sink, if one lies outside and one inside ($|\lambda_1| < 1 < |\lambda_2|$), a saddle, and if both lie outside, a source. Since

$$\lambda_1 \lambda_2 = \det(Df) = \alpha, \tag{13}$$

only sinks and saddles are obtained for $\alpha < 1$. If $\alpha = 1$ one finds centers and saddles. From equation (7) the eigenvalues are given by

$$\lambda_{1,2} = \tfrac{1}{2}\{(1+\alpha+\gamma s) \pm \sqrt{(1+\alpha+\gamma s)^2 - 4\alpha}\}, \qquad s = \sin(\bar{\phi} + \bar{v}). \tag{14}$$

Inserting $(\bar{\phi}_n, \bar{v}_n)$ from equation (10) one finds that the fixed points with $\bar{\phi}_n < \pi(\sin(\bar{\phi} + \bar{v}) > 0)$ are all saddle points of the first kind [16] while those with $\bar{\phi}_n > \pi(\sin(\bar{\phi} + \bar{v}) < 0)$ are sinks (centers) if

$$2n\pi(1-\alpha) < \gamma < 2\sqrt{n^2\pi^2(1-\alpha)^2 + (1+\alpha)^2}, \tag{15}$$

and saddles of the second kind [16] if

$$\gamma > 2\sqrt{n^2\pi^2(1-\alpha)^2 + (1+\alpha)^2}. \tag{16}$$

(Orbits approaching and leaving such a saddle do so in an oscillatory manner—such fixed points are sometimes called "reflection hyperbolic" in the physics literature.) The values

$$\gamma_n = 2n\pi(1-\alpha), \qquad \gamma_n' = 2\sqrt{n^2\pi^2(1-\alpha)^2 + (1+\alpha)^2} \tag{17}$$

are *bifurcation* values at the first of which a pair of fixed points appears in a saddle-node bifurcation [5, 16] and at the second of which a change of stability occurs. Such bifurcations are called *local* since they occur at a degenerate fixed point or periodic orbit. The next piece of analysis reveals that a period two motion appears at γ_n'. This second bifurcation is therefore a "flip".

Iterating f twice gives

$$\begin{aligned} \phi_{j+2} &= \phi_j + (1+\alpha)v_j - \gamma\cos(\phi_j + v_j), \\ v_{j+2} &= \alpha(\alpha v_j - \gamma\cos(\phi_j + v_j)) - \gamma\cos(\phi_j + (1+\alpha)v_j - \gamma\cos(\phi_j + v_j)), \end{aligned} \tag{18}$$

which leads to the following conditions for points of period 2, $(\hat{\phi}, \hat{v}) = f(f(\hat{\phi}, \hat{V}))$:

$$\gamma\cos(\hat{\phi} + \hat{v}) = (1+\alpha)\hat{v} + 2k\pi, \qquad \gamma\cos\hat{\phi} = -(1+\alpha)\hat{v} - 2k\pi\alpha, \qquad k = 0, \pm 1, \pm 2, \ldots. \tag{19, 20}$$

In the perfectly elastic case, $\alpha = 1$, equations (19) and (20) may be added to yield

$$\cos(\hat{\phi} + \hat{v}) + \cos\hat{\phi} = 0, \tag{21}$$

implying either

$$\cos(\hat{v}/2) = 0 \quad \text{or} \quad \cos(\hat{\phi} + \hat{v}/2) = 0, \tag{22}$$

and leading to points of period 2 with co-ordinates

$$(\hat{\phi}, \hat{v}) = (\arccos(-2(2m+k+1)\pi/\gamma), (2m-1)\pi), \tag{23}$$

and

$$(\hat{\phi}, \hat{v}) = (\tilde{\phi}, (2m+1)\pi - 2\tilde{\phi}), \tag{24a}$$

where $\phi = \tilde{\phi}$ is a solution of

$$\gamma\cos\phi = 2(2\phi - (2m+k+1)\pi). \tag{24b}$$

When $\alpha < 1$ the analysis is considerably more difficult and must be performed numerically. However, it is clear that equations (19) and (20) do not always have real solutions, and that new solutions appear as γ increases. It can now be shown that the value γ_n' of equation (17), at which one of the solutions $(\bar{\phi}_n, \bar{v}_n)$ loses stability, coincides with the appearance of a stable orbit of period two which bifurcates from $(\bar{\phi}_n, \bar{v}_n)$. One first sets $\phi = \bar{\phi}_n > \pi$ and $v = 2n\pi$ in equations (19) and (20). Using equation (10), one finds that k must be set equal to $-2n$ to study bifurcations from $(\bar{\phi}_n, \bar{v}_n)$. Doing this, and eliminating

$\hat{v}$ from equations (19) and (20), one obtains the equation

$$\gamma(\cos(\hat{\phi}+(4n\pi\alpha-\gamma\cos\hat{\phi})/(1+\alpha))+\cos\hat{\phi})+4n\pi(1-\alpha)=0. \tag{25}$$

A numerical study of this equation reveals that it has just two solutions (the fixed points of equation (10)) for $\gamma\in[\gamma_n,\gamma_n']$, no solutions for $\gamma<\gamma_n$ and four solutions for $\gamma>\gamma_n'$. Thus the bifurcation is supercritical, yielding a stable orbit of period two for $\gamma>\gamma_n'$. Subsequently this orbit becomes unstable at a third bifurcation value γ_n'' and a stable orbit of period four appears.

Moreover, as γ continues to increase, further pairs of period two orbits appear for each (fixed) value of n, as study of equation (25) reveals. Thus, for large γ one has orbits of both periods one and two, whose numbers grow indefinitely as $\gamma\to\infty$.

In principle one can go on to study orbits of higher periods but the computations rapidly become impractical. For example, one finds cascades of bifurcations to successively higher period orbits, and some aspects of this type of behavior will be described in section 5. Even in the case $\alpha=1$ approximations must be made to obtain workable results. Rather than continuing this analysis, the reader is referred to the papers of Greene [5] and Schmidt [18], in which bifurcations of periodic motions are studied in some detail. In the following sections a *global* analysis of the map is described which clarifies these *local* bifurcation results and enables one to assemble them into an overall picture.

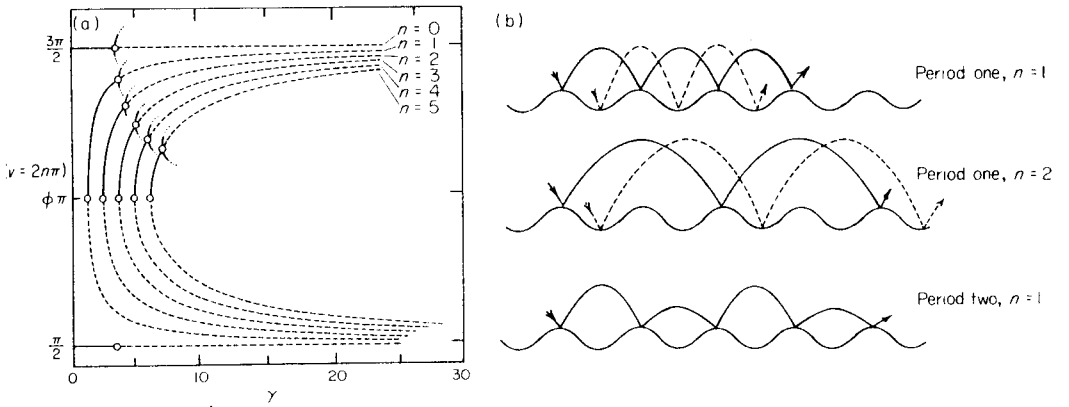

Figure 1. Period one and period two motions, $\alpha=0{\cdot}9$. The period two motions appear in flip bifurcations at $\gamma=\gamma_n'$. (a) Bifurcation diagram; (b) physical motions. ——, Stable period one; – – –, unstable period one; ···—···, stable period two.

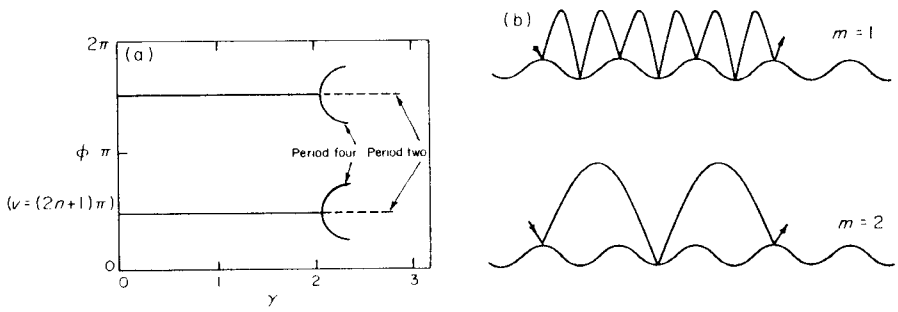

Figure 2. Examples of other period two motions, which exist for all values of γ, $\alpha=1$. These bifurcate to period four at $\gamma=2$. (a) Bifurcation diagram; (b) physical motions.

Before starting the global analysis, however, it is useful to discuss some of the periodic orbits in more detail and comment on their physical significance. Results are presented graphically. Figure 1 is a bifurcation diagram showing the period one and some of the period two motions; note that there are two families of the latter motions and here only those that arise in period doubling bifurcations, as discussed above are shown. In Figure 2, for the case $\alpha = 1$ some members of the second family of period two orbits are shown, and also the physical motions associated with some of these orbits.

3. THE EXISTENCE OF HORSESHOES

In 1963 Smale [19] gave an example of a two dimensional diffeomorphism with infinitely many periodic points. His example was inspired by results of Levinson [20] on a version of the forced van der Pol equation. Subsequently such motions were proven to occur in this equation by Levi [21] and a similar diffeomorphism was found in the Poincaré maps [2] associated with other forced non-linear oscillators [12–15]. Smale's diffeomorphism has been named the *horseshoe*, since it deforms a rectangle in the state space into the shape of a horseshoe (cf. Figures 3 and 5, below). Subsequently Moser [22] provided explicit criteria which, if met, guarantee the existence of horseshoes in specific maps. In this section it is verified that the map (5) meets these conditions for sufficiently large γ and α sufficiently close to one. This section is somewhat technical and the reader may prefer to glance at the figures and the main result and then go directly to section 4 where the horseshoe map is described in more general terms.

Moser's results [22] are as follows. Given the unit square $Q = [0, 1] \times [0, 1]$ in the (x, y) plane a *horizontal strip* is a set $\{(x, y) | x \in [0, 1],\ y \in [h_1(x),\ h_2(x)]\}$ where $h_i(x)$, $i = 1, 2$ are horizontal curves: i.e., $|h_i(x_1) - h_i(x_2)| \leq \mu |x_1 - x_2|$ for some $0 < \mu < 1$. Similarly a *vertical strip* is bounded by curves $x = v_i(y)$ where $|v_i(y_1) - v_i(y_2)| \leq \mu |y_1 - y_2|$. The assumptions A1 and A2 for the map $f: Q \to \mathbb{R}^2$ are as follows.

A1. Let H_i, V_i, $i = 1, 2$, be disjoint horizontal and vertical strips respectively and let $f(H_i) = V_i$.

A2. There exist sector bundles $S^u = \{(\xi, \eta) | |\xi| < \mu |\eta|\}$ defined over $V_1 \cup V_2$ and $S^s = \{(\xi, \eta) | |\eta| < \mu |\xi|\}$ defined over $H_1 \cup H_2$ with $0 < \mu < 1$ such that $Df(S^u) \subset S^u$ and $Df^{-1}(S^s) \subset S^s$. Moreover, if $Df(\xi_0, \eta_0) = (\xi_1, \eta_1)$ and $Df^{-1}(\xi_0, \eta_0) = (\eta_{-1}, \xi_{-1})$ then $|\eta_1| > (1/\mu)|\eta_0|$ and $|\xi_{-1}| > (1/\mu)|\xi_0|$. The second condition implies that f and its linearization Df expand vertical distances and contract horizontal ones in a controlled manner. (Actually it is sufficient that A2 hold on $(V_1 \cup V_2) \cap (H_1 \cup H_2)$, since the invariant set one seeks is confined to these four squares—this fact is used later.)

Under these two assumptions, Moser proved that f possesses a horseshoe, or, more precisely, that there is an invariant set Λ for f such that f restricted to $\Lambda (f|_\Lambda)$ is homeomorphic to a shift on an alphabet of two symbols. The shift is explained in section 4, and Moser's theorem given below, after verification of A1 and A2 for the particular map of interest here.

One starts by demonstrating the existence of pairs of disjoint "horizontal" and "vertical" strips H_i, V_i, $i = 1, 2$, such that $f(H_i) = V_i$. One then estimates conditions on the derivatives Df, Df^{-1} of the map f and its inverse restricted to H_i and V_i. The satisfaction of these latter conditions guarantees that the non-wandering set Λ is hyperbolic [2] and hence stable to small perturbations in the map.

LEMMA 1. *For $\alpha = 1$ and $\gamma \geq 4\pi$ the map f possesses a topological horseshoe: i.e., there are "horizontal" and "vertical" strips H_i, V_i, such that $f(H_i) = V_i$, $i = 1, 2$.*

Here a "horizontal" strip is understood to be bounded by curves $v = v(\phi)$ with $|v'| < 2$ and a "vertical" strip is bounded by curves $\phi = \phi(v)$ with $|\phi'| < 1/2$ (the ideal situation of Moser's result rarely occurs in practice!).

Proof. Note that, for $\alpha = 1$, f is periodic in both ϕ and v with period 2π. Without loss of generality, one may pick as basic domain Q the parallelogram $ABCD$ bounded by the lines $\phi + v = 0$ (AB), $\phi + v = 2\pi$ (CD), $\phi = 0$ (AD), $\phi = 2\pi$ (BC) (see Figure 3).

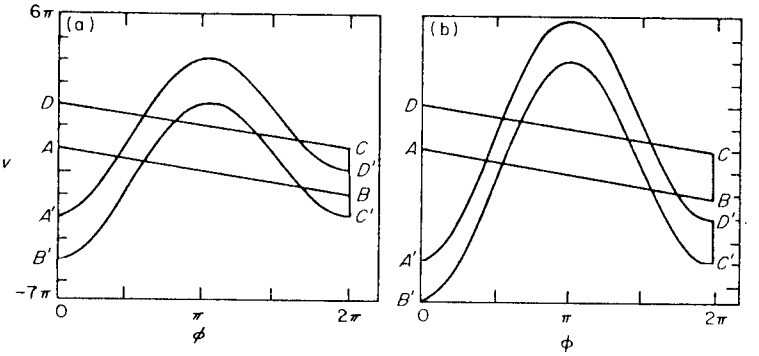

Figure 3. The creation of horseshoes as γ increases for the area preserving case, $\alpha = 1$. The points A, B, C, D are mapped to A', B', C', D'. (a) $\gamma = 3\pi$; (b) $\gamma = 5\pi$.

Note that Q is foliated by the family of lines $\phi + v = k$, $k \in [0, 2\pi]$ and that the images of such lines under f are vertical lines $\phi = k$, $v \in [k - 2\pi - \gamma \cos k,\ k - \gamma \cos k]$. Finally, the images of the boundaries $\phi = 0$ and $\phi = 2\pi$ are curves $v = \phi - \gamma \cos \phi$, $v = \phi - 2\pi - \gamma \cos \phi$.

To obtain the required disjoint strips it is sufficient to ensure that $A'D'$, the image of AD (the boundary $\phi = 0$), intersects AB $(\phi + v = 0)$ in two distinct points. $A'D'$ is given by $v = \phi - \gamma \cos \phi$ and AB by $v = -\phi$ and thus one requires that

$$\gamma \cos \phi = 2\phi \tag{26}$$

has two distinct roots in $(0, 2\pi)$. It is easy to see that there are precisely two such roots provided that $\gamma \geq 4\pi$. Moreover, simple computations reveal that, for $\gamma \geq 4\pi$, the slopes of the curves bounding V_1 and V_2 are less in magnitude than $\frac{1}{2}$ and those bounding H_1 and H_2 less in magnitude than 2.

Remark 1. More delicate estimates reveal that γ can be somewhat reduced without destroying the topology of the strips.

Remark 2. Since the images $A'D'$ and $B'C'$ of AD and BC are given by $v = \phi - \gamma \cos \phi$ and $v = \phi - 2\pi - \gamma \cos \phi$ respectively it is easy to compute bounds between which the vertical strips V_1 and V_2 must lie. They are given by the appropriate roots of the following equations:

$$V_1\text{: roots of } \phi - \gamma \cos \phi = -\phi \text{ and } \phi - 2\pi - \gamma \cos \phi = 2\pi - \phi \text{ between 0 and } \pi, \tag{27}$$

$$V_2\text{: roots of } \phi - 2\pi - \gamma \cos \phi = 2\pi - \phi \text{ and } \phi - \gamma \cos \phi = -\phi \text{ between } \pi \text{ and } 2\pi. \tag{28}$$

It is easy to see that, as γ increases, these roots converge on $\pi/2$ and $3\pi/2$ respectively, and thus that the widths of V_1 and V_2 decrease with increase of γ. For example, solutions of equations (27) and (28) show that, for $\gamma = 5\pi$, the ϕ co-ordinates of points in V_1 and V_2 lie in the intervals (1·39, 2·13) and (4·48, 5·49) respectively. Using the inverse map

f^{-1} one finds that the corresponding horizontal strips H_1, H_2 are similarly bounded by $\phi + v = 1{\cdot}39$, $2{\cdot}13$ and $4{\cdot}48$, $5{\cdot}49$ (all co-ordinates are given in radians).

LEMMA 2. *For γ sufficiently large (5π is sufficient), there are sector bundles $S^u(p)$, $S^s(p)$ based at points $p \in \bigcup_{i,j=1,2}(H_i \cap V_j)$ centered on lines $\phi = \text{const}$ and $\phi + v = \text{const}$ respectively and each of angular extent $\pi/4$, such that $Df(S^u(p)) \subset S^u(p)$ and $Df^{-1}(S^s(p)) \subset S^s(p)$. Moreover, $Df(p)$ expands vertical distances by a factor of at least $5{\cdot}5$ and Df^{-1} expands "horizontal" distances by a factor of at least $4{\cdot}5$.*

Remark. Here, lines $\phi + v = \text{const.}$ are termed "horizontal".

Proof. Linearizing the map, one has

$$Df\begin{bmatrix} 1 & 1 \\ s & 1+s \end{bmatrix}, \quad Df^{-1}\begin{bmatrix} 1+s & -1 \\ -s & 1 \end{bmatrix}, \tag{29}$$

where $s = \gamma \sin(\phi + v)$ or $\gamma \sin \phi$ respectively. From the estimates above, for $\gamma \geq 5\pi$ one has $\phi + v \in (1{\cdot}39,\ 2{\cdot}13) \cup (4{\cdot}48,\ 5{\cdot}49)$ for $p \in H_1 \cup H_2$ and similar bounds for ϕ for $p \in V_1 \cup V_2$. This shows that $|\sin(\phi + v)|, |\sin \phi| > 0{\cdot}716$ for points $p \in \bigcup_{i,j=1,2}(H_i \cap V_j)$, or $|\gamma \sin(\phi + v)|, |\gamma \sin \phi| > 11{\cdot}24$.

Only the estimate for sector S^u need be considered here since that for S^s is obtained similarly. Consider the image of the sector S^u shown in Figure 4 under the map Df. Let

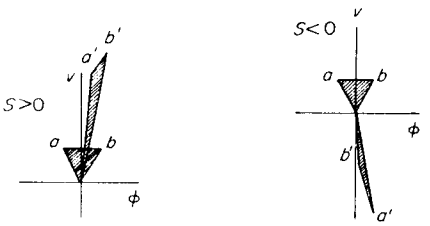

Figure 4. The vertical sector bundles S^u and their images under Df.

the "corners" of S^u be given by the points $(\pm 0{\cdot}414, 1)$ $(\tan \pi/8 \approx 0{\cdot}414)$. Taking $s = 11{\cdot}24$ one obtains the images $(1{\cdot}414, 16{\cdot}89)$, $(0{\cdot}586, 7{\cdot}587)$ respectively and taking $s = -11{\cdot}24$ one obtains $(1{\cdot}414, -14{\cdot}893)$, $(0{\cdot}586, -5{\cdot}587)$ respectively. Since $|s| = |\gamma \sin(\phi + v)| > 11{\cdot}24$ for points $p \in H_i \cap V_j$ and increases of $|s|$ make the images of the sectors even larger and thinner, the estimate is obtained.

The computation for "horizontal" sectors, bounded by lines of angle $-\pi/8$, $-3\pi/8$, is slightly more awkward but proceeds in a similar manner. One ends by noting that, for $\gamma > 5\pi$, $|\gamma \sin(\phi + v)|, |\gamma \sin \phi| > 11{\cdot}24$ and thus that the estimates hold for all $\gamma > 5\pi$.

These two lemmas establish the conditions of Moser's assumptions 1 and 3 ([22], Chapter 3). Here in the choice of sectors Moser's parameter μ has been taken as $\mu = \tan \pi/8 \approx 0{\cdot}414$. The sector bundle estimates guarantee that f maps vertical strips to vertical strips with a contraction of at least $\nu = \mu/(1-\mu) \approx 0{\cdot}706$ and that f^{-1} maps horizontal strips with a similar contraction.

These facts, together with the fact that, for $\alpha = 1$, $\det(Df) = \det(Df^{-1}) = 1 < 1/2\mu^2 \approx 2{\cdot}917$, imply the following.

THEOREM 3. *For $\gamma \geq 5\pi$ and $\alpha = 1$ the map* (5) *possesses a zero dimensional, invariant, hyperbolic, Cantor set Λ. The map f restricted to Λ is homeomorphic to the shift on two symbols.*

The hyperbolic structure of Λ, and its structural stability, imply that the theorem also holds for $\alpha \neq 1$, but sufficiently close to 1. Thus it follows that one has a complicated invariant set Λ_α, possessing countably many periodic orbits of all periods and uncountably many bounded non-periodic motions, even in the weakly dissipative case. (Improved estimates on the relative values of γ and $\alpha \neq 1$ for which one obtains a horseshoe could easily be obtained by the methods used in this section.) However, when $\alpha \neq 1$ the map is not periodic in v and then the image of each strip in the (ϕ, v) phase cylinder, bounded by $\phi + v = 2(n+1)\pi$, $\phi + v = 2n\pi$ is no longer a simple translation of that of the basic strip bounded by $\phi + v = 2\pi$, $\phi + v = 0$. This is taken up in section 5.

4. THE IMPLICATIONS OF HORSESHOES

This section is concerned with a simple piecewise linear mapping which retains all the important qualitative features of the horseshoe map defined on the strips H_i. The exposition is partially taken from the works of Chillingworth [2], Moser [22], Nitecki [23] and Newhouse [24], following the original work of Smale [19]. For the unit square $Q = [0, 1] \times [0, 1]$ consider the map F: $Q \to \mathbb{R}^2$ defined such that

$$F([0, 1]\times[0, \nu]) = [0, \mu]\times[0, 1], F([0, 1]\times[1-\nu, 1]) = [1-\mu, 1]\times[0, 1], 0 < \mu < \nu < 1/2, \tag{30}$$

where the horizontal and vertical strips are

$$\begin{aligned} H_1 &= [0, 1]\times[0, \nu], \qquad V_1 = [0, \mu]\times[0, 1], \\ H_2 &= [0, 1]\times[1-\nu, 1], \qquad V_2 = [1-\mu, 1]\times[0, 1]. \end{aligned} \tag{31}$$

F is assumed to be linear on H_1 and H_2, with

$$DF(p) = \begin{bmatrix} \mu & 0 \\ 0 & 1/\nu \end{bmatrix} \text{ for } p \in H_1, \qquad DF(p) = \begin{bmatrix} -\mu & 0 \\ 0 & -1/\nu \end{bmatrix} \text{ for } p \in H_2, \tag{32}$$

and $F([0, 1]\times(\nu, 1-\nu))$ is assumed to lie outside Q (see Figure 5).

The non-wandering set Λ_v of points which remain in Q for all backward iterates of F is given by

$$\Lambda_v = \bigcap_{k=0} F^k(Q) = Q \cap F(Q) \cap F^2(Q) \cap \ldots. \tag{33}$$

$Q \cap F(Q)$ is precisely the pair of vertical strips $V_1 \cup V_2$ of Figure 5. The image of each of these itself intersects Q in a pair of strips: cf. Figure 5(b). The reader will not find it

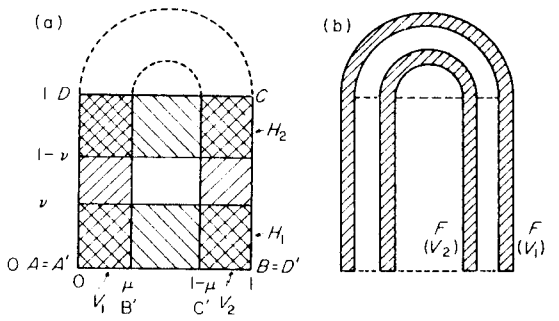

Figure 5. A piecewise linear horseshoe. (a) $Q \cap F(Q)$; (b) $F(Q \cap F(Q))$.

difficult to verify that $\bigcap_{k=0}^{n} F^k(Q)$ consists of 2^n vertical strips each of width μ^n and thus in the limit one obtains an uncountable set of vertical lines, since $(2\mu)^n \to 0$ as $n \to \infty$. Hence $\Lambda_v = C_v \times [0, 1]$, where C_v is the Cantor set obtained by removing the middle fraction $\delta_v = (1-2\mu)$ of the horizontal interval [0, 1], followed by the middle δ_v of the remaining closed intervals, *ad infinitum*. Similarly one finds that Λ_h, the set of points remaining in Q for all forward iterates of F, is given by $\Lambda_h = [0, 1] \times C_h$, where C_h is the middle $\delta_h = (1-2\nu)$ Cantor set of the vertical interval. Thus the non-wandering set of points which *never* leave Q is given by $\Lambda = \Lambda_h \cap \Lambda_v = C_h \times C_v$, and is itself a Cantor set.

One can label each of the points $p \in \Lambda$ with a doubly infinite symbol sequence $\{a_n(p)\} = \{\ldots a_{-2}(p)a_{-1}(p) \cdot a_0(p)a_1(p)a_2(p)\ldots\}$ as follows. The forward going sequence $a_0a_1a_2\ldots$ locates p in one of the horizontal lines of Λ_h and the backward going sequence $a_{-1}a_{-2}\ldots$ locates p in one of the vertical lines of Λ_v. For example $a_0 = 1$ if $p \in H_1$ and $a_0 = 2$ if $p \in H_2$; similarly $a_{-1} = 1$ (resp. 2) if $p \in V_1$ (resp. V_2). It can be shown that there is precisely one such symbol sequence for each point in Λ. Moreover, the sequences can be chosen to reflect the dynamics of F restricted to $\Lambda(F|_\Lambda)$, by requiring that

$$\{a_n(F(p))\} = \sigma\{a_n(p)\}, \tag{34}$$

where σ is the shift operation defined by

$$(\sigma\{a_n\})_k = a_{k+1}: \tag{35}$$

i.e., a shift of the sequence one place to the left (or of the decimal point one place to the right).

The space Σ of two symbol sequences has a natural topology based on the fact that two sequences $\{a_n(p)\}$, $\{a_n(q)\}$ are $1/N$ close if $a_n(p) = a_n(q)$ for all $|n| \leq N$. This in turn implies that the points p and q lie within a rectangle with height ν^N and width μ^N. By using these ideas it is possible to prove that the map $F|_\Lambda$ is *homeomorphic* to the shift $\sigma: \Sigma \to \Sigma$, and thus that an analysis of the *symbolic dynamics* of F via σ is possible. One can use this to prove various facts (cf. reference [2]).

PROPOSITION 4. *The invariant set Λ contains (a) a countable set of periodic orbits of all periods, (b) an uncountable set of non-periodic motions, (c) a dense orbit, and (d) the periodic orbits are all of saddle type and they are dense in Λ.*

The countable set of periodic orbits follows from the fact that one can enumerate all periodic sequences $(\ldots 111 \cdot 111\ldots;\ \ldots 222 \cdot 222\ldots;\ 1212 \cdot 1212\ldots;$ $\ldots 122 \cdot 122\ldots;\ldots 112 \cdot 112\ldots$; etc.) and to each of these there corresponds a periodic orbit of F. One can even count the periodic orbits of a given period: (b) follows because there is still an uncountable point set left when all periodic points are removed. The set of periodic orbits is dense because any orbit can be approximated arbitrarily closely by a periodic orbit. A dense orbit is constructed by joining all possible finite symbol sequences end to end. Finally, the stability of a periodic orbit $\{p_j\}$ of period k is given by $DF^k = DF(p_k)DF(p_{k-1})\ldots DF(p_1)$, and hence

$$DF^k = \begin{bmatrix} \pm\mu & 0 \\ 0 & \pm 1/\nu \end{bmatrix}^k = \begin{bmatrix} \pm\mu^k & 0 \\ 0 & 1/\nu^k \end{bmatrix}, \tag{36}$$

which has eigenvalues $0 < |\mu^k| < 1 < |1/\nu^k|$. Half (roughly) of these periodic points are saddles of the first kind and half saddles of the second kind.

While the set Λ is extremely complicated and contains an uncountable infinity of non-periodic or "chaotic" orbits, it is not an attractor. It can, however, exert a dramatic influence on the behavior of typical orbits which pass close to it since the stable manifold

$W^s(\Lambda)$, or set of orbits $f^n(q)$ asymptotic to Λ as $n \to \infty$, behaves like an uncountable set of saddle separatrices. (In fact locally this stable manifold is just Λ_h: the product of an interval and a Cantor set.) One therefore expects orbits passing near Λ to display an extremely sensitive dependence upon initial conditions, and exhibit a transient period of chaos before perhaps setting down to a stable periodic orbit. Recall that such orbits can co-exist with the horseshoe since only the image under f of a specially chosen domain of the state space has been considered. However, in the next section it is argued that even stable periodic orbits may have arbitrarily long periods, and hence may appear as erratic as the genuinely non-periodic motions.

5. BIFURCATION TO HORSESHOES AND CHAOTIC MOTIONS

In this section the behavior of the map $f_{\alpha,\gamma}$ as γ is increased for fixed $\alpha < 1$ is considered. Specifically, a region Q bounded by the lines $\phi = 0$, $\phi = 2\pi$, $\phi + v = 2n\pi$, $\phi + v = (2n+2)\pi$ is fixed and chosen such that $f_{\alpha,0}(Q)$ lies entirely below Q; see Figure 6(a). As γ is

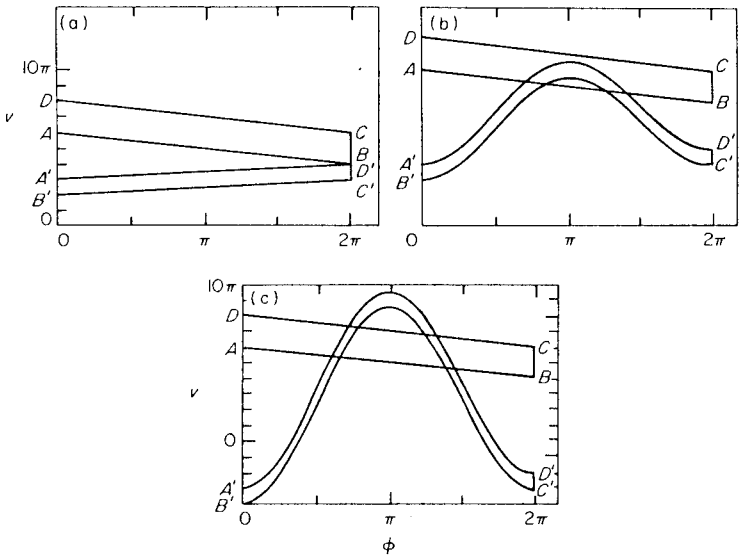

Figure 6. The creation of a horseshoe; $\alpha = 0{\cdot}5$, $n = 3$. (a) $\gamma = 0$; (b) $\gamma = 3\pi = \gamma_n$; (c) $\gamma = 6\pi > \gamma_n^h$.

increased, the center of the image of Q rises until the image of the horizontal line AC ($\phi = 2n\pi$), given by $v = \alpha v - \gamma \cos v$, just touches AC at the point $(\phi, v) = (\pi, 2n\pi)$; see Figure 6(b). This occurs when $\gamma = \gamma_n = 2n\pi(1-\alpha)$ and is, of course, the saddle node bifurcation point for the pair of fixed points lying on $v = 2n\pi$ which was found in section 2. One already knows that the sink bifurcates to a sink of period two at $\gamma_n' = 2\sqrt{n^2\pi^2(1-\alpha)^2 + (1+\alpha)^2}$. One can now conclude that an infinite sequence of further bifurcations must occur between γ_n' and γ_n^h, the critical value at which the horseshoe is created (see Figure 6(c)), since for $\gamma \geq \gamma_n^h$ there is a countable infinity of periodic orbits, including orbits of arbitrarily long periods, in Q. The question of the order in which these bifurcations occurs for such maps is still open and appears to depend on the dissipation parameter α.

In the limit $\alpha \to 0$ the map $f_{\alpha,\gamma}$ tends to the singular map

$$f_{0,\gamma}: (\phi, v) \mapsto (\phi + v, -\gamma \cos(\phi + v)), \tag{37}$$

which shrinks areas to zero in one iterate. Since each line $\phi + v = c$ is shrunk to a point $(c, -\gamma \cos c)$ by $f_{0,\gamma}$ one can set $\phi = 0$ (say) and consider the one dimensional (non-invertible) map

$$v \mapsto -\gamma \cos v, \tag{38}$$

which takes an interval, stretches and folds it repeatedly, and maps it into $[-\gamma, \gamma]$. Near any maximum this resembles a quadratic map of the form

$$v \mapsto \gamma - v^2/2, \tag{39a}$$

or, equivalently,

$$v \mapsto \bar{\gamma} v(1 - v), \tag{39b}$$

which has been studied extensively and shown to exhibit startlingly complex behavior, including countable sequences of period doubling bifurcations (cf. the publications of Stefan [25], Guckenheimer [26], Collet, Eckmann and Lanford [27], and Collet and Eckmann [28]). However, the work of Newhouse [24, 29] and of Gavrilov and Silnikov [30] (cf. the article by Greenspan and Holmes [15]) implies that the typical behavior for the two dimensional diffeomorphism ($\alpha \neq 0$) is yet more complex, since such maps can possess countably infinite sets of *stable* periodic orbits for selected parameter values in addition to the saddle type orbits discussed in section 4, while one dimensional maps such as mapping (38) can have at most finite sets of stable periodic orbits (a map with a single maximum, such as mapping (39), can have at most one stable orbit for each parameter value [28]).

The studies contained in the literature cited above do not provide a complete characterization of the bifurcation behavior in each "n band" as γ varies between γ_n^l and γ_n^h, but they do show that stable periodic motions of arbitrarily long period are created in saddle-node bifurcations and subsequently double their periods repeatedly as γ increases. Thus, stable orbits with periods longer than any preassigned period can be found; such orbits are indistinguishable in practice from the bounded non-periodic motions of the horseshoe, but their stability renders them observable. Newhouse [29] has suggested that such orbits may constitute the hypothetical "strange attractor" observed by Hénon [31] and many others in numerical iterations of two dimensional maps.

In the present case numerical iterations of equation (5) reveals similar complex orbits. Figure 7 shows a sequence of phase portraits (= orbits) for α (= 0·8) fixed and several values of γ. The stable sink of (a) has bifurcated to an orbit of period two in (b) and successively more complex orbits are seen in (c) and (d). In each case the initial conditions were chosen to be near $v = 2\pi$, and, while the orbit remains close to the $n = 1$ band for low values of γ (see (a) and (b)), for higher values it leaves the band and wanders erratically over a bounded subset of the state cylinder before setting down to a stable orbit (c), or apparently continues to wander (d). In (c) 500 iterates were required before the asymptotic behavior became clear; in (d) 5000 iterates were computed. Note that the orbits of (c) and (d) do not correspond to physical motions of the bouncing ball since the departure velocity V becomes negative. These chaotic motions are, however, of considerable mathematical interest.

Figure 8 illustrates the condition necessary (but not sufficient) for this wandering to occur. It shows partial boundaries of the domain of attraction of the period one sink in the $n = 1$ band formed by the stable manifolds of the associated saddle point. Finite segments of these manifolds are easily computed by iterating a short interval of the stable eigenvector of the linearized map (7) containing the saddle point, under the inverse map (6). The unstable manifold may similarly be found by iterating an interval of the

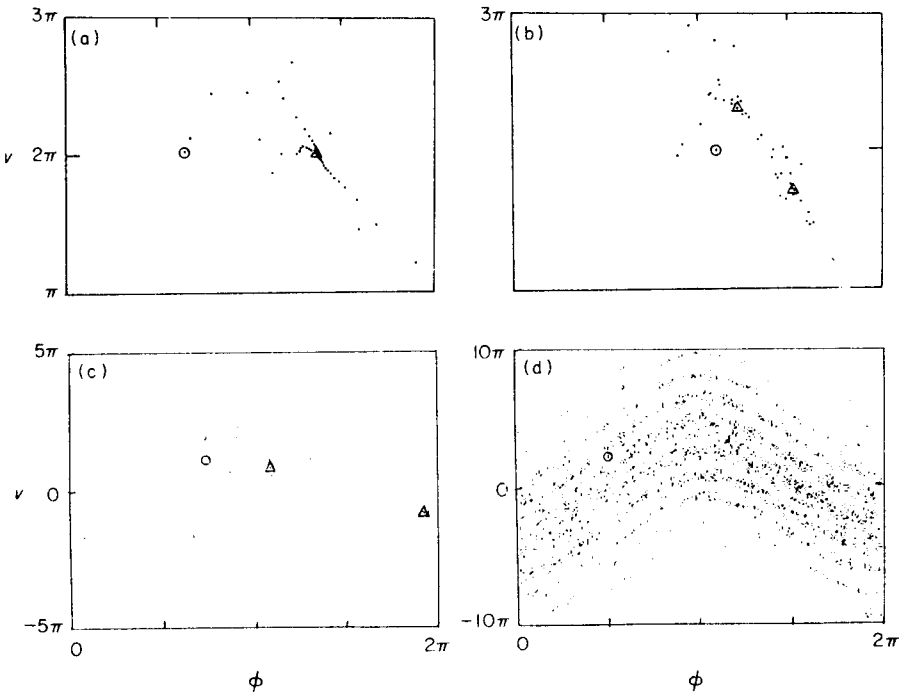

Figure 7. Orbits of $f_{\alpha,\gamma}$; $\alpha = 0{\cdot}8$. ⊙, Initial condition, △, asymptotic limit of orbit. The $n = 1$ period two motion appears for $\gamma \approx 3{\cdot}813022$. (a) $\gamma = 3$; (b) $\gamma = 4$; (c) $\gamma = 5$; (d) $\gamma = 10$. No periodic limit apparent after 5000 iterates.

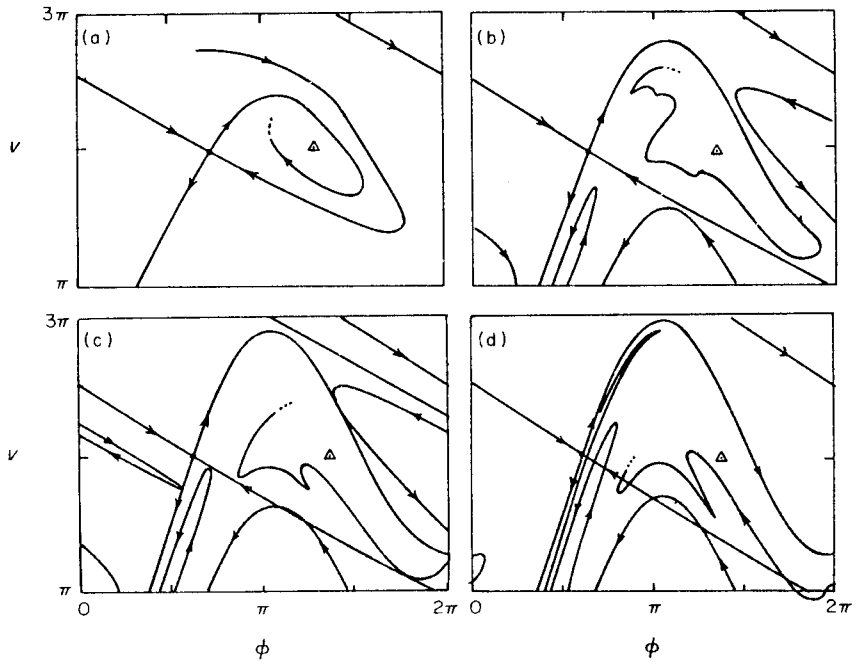

Figure 8. Stable and unstable manifolds of the $n = 1$ saddle point. The $n = 1$ sink is denoted by △. (a) $\gamma = 2$; (b) $\gamma = 3$; (c) $\gamma = 3{\cdot}28$: first tangency; (d) $\gamma = 3{\cdot}5$: transverse homoclinic orbits.

unstable eigenvector under the map (5) (cf. [32]). When transverse intersections of stable and unstable manifolds exist, as in Figure 8(d), it is very difficult to predict the asymptotic behavior of an orbit unless the initial conditions are known extremely accurately, since any two orbits starting on different sides of the stable manifold will ultimately separate exponentially fast. The violent winding of this manifold implies that the domains of attraction have complicated boundaries with infinitely many long thin "tongues" penetrating close to other attracting orbits (cf. reference [32]).

Note that intersections of manifolds in the $n = 1$ band occur for values of γ for which the sink at $(\bar{\phi}_1, \bar{v}_1) = (\arccos(2\pi(\alpha - 1)/\gamma), 2\pi)$ is still stable, and far below γ_1^h, the value at which the $n = 1$ horseshoe appears. However the global bifurcation occurring when the manifolds are tangent (Figure 8(c)) reproduces "in miniature" all the behavior associated with the creation of horseshoes of Figure 6. Consider the simplified sketch of the manifolds in Figure 9. One can select a small rectangle, Q^N, such that, for some

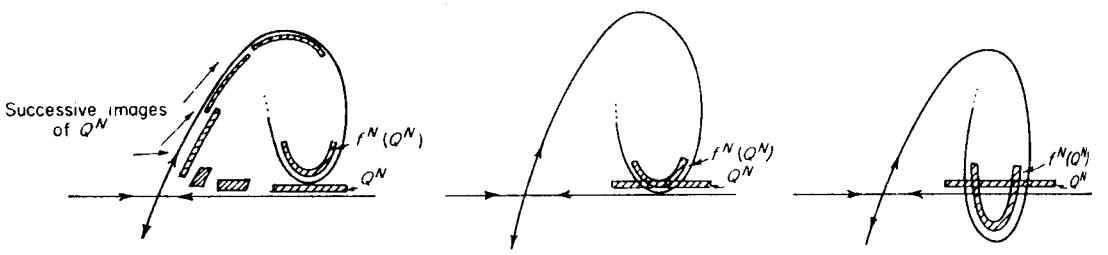

Figure 9. The creation of mini-horseshoes for $f^N_{\alpha,\gamma}$.

fixed iterate N of the map, $f^N_{\alpha,\gamma}(Q^N)$ lies as shown respectively before (a), at (b) and after (c) the tangency (cf. references [15, 24, 29, 30]). Thus, on a suitably chosen rectangle, $f^N_{\alpha,\gamma}$ has horseshoes once transverse homoclinic points exist. The stable manifolds belonging to the countable set of saddle type orbits within these horseshoes wind around close to the stable manifolds of the saddle point shown in Figure 8(d), further complicating the structure of the domain of attraction. By taking all integers $M > N$, countably many such rectangles Q^M, each with its horseshoe, can be found, so that even if a low period stable orbit exists somewhere in the phase space, and initial conditions are chosen in its domain of attraction, the orbit may behave in a chaotic manner for a long time before finally "settling down" to the periodic attractor. In a similar map Lieberman has noted instances of apparent chaos for as many as 50 000 iterates before the appearance of a stable period three motion [33]. In view of this, the complex orbits of figures 7(c) and (d) are not surprising.

In the present problem, as in many others (cf. references [11, 12, 15, 31]) there appear to be parameter values for which orbits are *never* asymptotic to periodic attractors. Figure 10(a) is an illustration of such an orbit, which had not displayed any recognizable asymptotic behavior after 60 000 iterates. Note, however, that the orbit does exhibit a striking global structure in that it appears to fall on a set of curves. Magnification of regions of the phase space suggest that, as in Hénon's work [31], this set is not finite (Figure 10(b)), but is locally the product of a smooth curve and a Cantor set. This is precisely the structure of the closure of the unstable manifolds of the horseshoes, or, indeed, of the periodic orbits within them. (Locally, this is just the set Λ_v described in section 4.) In Figure 10(c) a portion of the unstable manifold of the saddle point at $(\phi, v) = (\pi/2, 0)$ is shown. Comparing this with Figure 10(a) makes it clear that the orbit seems to approach or to lie on this manifold. In fact if the bounded set $A = \{\phi, v \mid |v| < 8\pi\}$

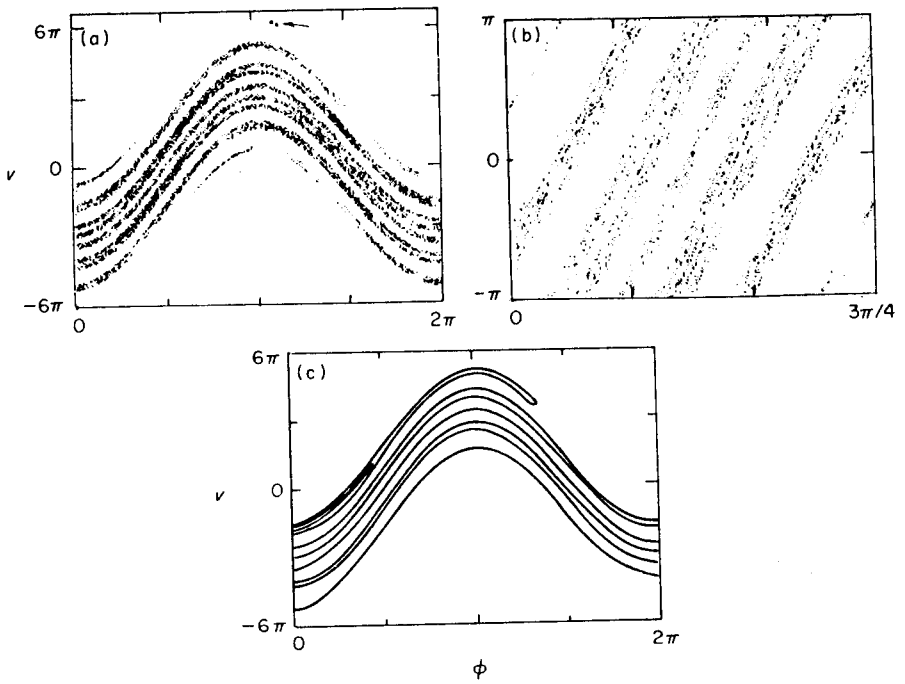

Figure 10. The "strange attractor". (a) 60 000 iterates of a point near $(\pi/2, 0)$; (b) enlargement of part of (a); (c) the unstable manifold of $(\pi/2, 0)$.

is taken in this case ($\alpha = 0{\cdot}5$, $\gamma = 10$) it can be shown by the methods of section 2 (equation (9)) that $f_{\alpha,\gamma}(A)$ is contained in A. Moreover, the attracting set A defined as the intersection of all forward images of A,

$$A = \bigcap_{n=0}^{\infty} f^n_{\alpha,\gamma}(A), \tag{40}$$

is equal to the closure of the unstable manifold of the saddle point at $(\pi/2, 0)$. This attracting set may, however, contain stable periodic orbits whose domains of attraction are so thin and contorted that they are effectively unobservable due to numerical errors (cf. reference [15], section 6.3).

This "strange attractor" coexists with a stable orbit of period two in the $n = 3$ band near the fixed point at $(\bar{\phi}, \bar{v}) = (\arccos(6\pi(\alpha - 1)/\gamma), 6\pi)$; see Figure 10(a). The domain of attraction of this motion winds back and forth in the "gaps" in the other attractor.

6. CONCLUSIONS AND PHYSICAL IMPLICATIONS

Although the complex motions discussed in the preceding section, and the bifurcations leading to them, are not fully understood one can draw some useful physical conclusions from this incomplete analysis.

The existence of horseshoes in the bands above $v = 0$, both on a global scale, as shown in section 3, and in miniature, as shown in section 5 (Figure 9) implies that countably infinite sets of unstable periodic motions of arbitrarily long period as well as non-periodic motions exist, provided that γ exceeds a certain limit, which can be estimated as in section 3 or easily found numerically, by looking for intersections of manifolds, as in section 5. Moreover Newhouse's work implies that, for a residual set of parameter values

near those at which tangencies of manifolds occur, there are countable sets of *stable* periodic motions of arbitrarily long period, while finite sets of such motions exist for open sets of parameter values. These observations together imply that stable (observable) motions of almost any degree of irregularity occur, since one can find periodic attractors whose periods exceed any specified number of iterates. Moreover, the size, shape and mutual interweaving of the domains of attraction of any such periodic motions implies that orbits will exhibit an extremely sensitive dependence on initial conditions, even when they do eventually approach a simple low period orbit.

As noted in section 5, the stable high period orbits cannot always be realized numerically, and thus may also be physically unobservable. Instead, one can expect to see sustained, bounded, chaotic motions of the ball, which have their mathematical analogue in bounded non-periodic orbits which remain above $v = 0$. This goes some way towards explaining the experimental results of Wood and Byrne [1] mentioned in section 1.

A number of other impact governed problems, such as that of mechanical linkages with free play, are described by models similar to the present one. One therefore expects to observe chaotic responses to deterministic (periodic) excitations in those cases also. Since such mechanisms play an important role in the generation of industrial noise and vibration [1], it is of interest to study their dynamics both from a geometrical viewpoint, as in this paper, and from a probabilistic viewpoint. In reference [1], probability density functions for departure velocity $V(t)$ were computed for given (Gaussian) excitations $W(t)$. An examination of Figure 10(a) suggests that an "effective density function" might be sought for the present, deterministic case, since the motion is effectively random, the initial condition being rapidly "forgotten" due to the exponential separation of neighboring orbits. Recently some work has been done in this area for the dissipative Chirkov-Taylor map, which is identical to equation (5) under a simple linear change of co-ordinates. The interested reader should refer to the papers of Jensen and Oberman [34, 35] and the references therein.

REFERENCES

1. L. A. WOOD and K. P. BYRNE 1981 *Journal of Sound and Vibration* **78**, 329–345. Analysis of a random repeated impact process.
2. D. R. J. CHILLINGWORTH 1976 *Differentiable Topology with a View to Applications*. London: Pitman Press.
3. J. B. TAYLOR 1968 Unpublished notes (see reference [5]).
4. B. V. CHIRIKOV 1979 *Physics Reports* **52**, 265–379. A universal instability of many-dimensional oscillator systems.
5. J. M. GREENE 1979 *Journal of Mathematical Physics* **20**, 1183–1201. Method for determining a stochastic transition.
6. A. LICHTENBERG, M. A. LIEBERMAN and R. H. COHEN 1980 *Physica* **1D**, 291–305. Fermi acceleration revisited.
7. L. D. PUSTYLNIKOV 1972 *Soviet Mathematics Doklady* **13**, 36–38. On stability of half-trajectories under area preserving mappings of the plane.
8. L. D. PUSTYLNIKOV 1972 *Soviet Mathematics Doklady* **13**, 94–97. Existence of a set of positive measure of oscillating motions in a certain problem of dynamics.
9. L. D. PUSTYLNIKOV 1978 *Transactions of the Moscow Mathematical Society* **14**, 1–101. Stable and oscillating motions in non-autonomous dynamical systems.
10. A. LICHTENBERG and M. A. LIEBERMAN 1981 *Regular and Stochastic Motion*. Berlin, Heidelberg, New York: Springer Verlag (to appear).
11. B. V. CHIRIKOV and F. M. IZRAELEV 1981 *Physica* **2D**, 30–37. Degeneration of turbulence in simple systems.
12. P. J. HOLMES 1979 *Philosophical Transactions of the Royal Society* **A292**, 419–448. A nonlinear oscillator with a strange attractor.

13. F. C. MOON and P. J. HOLMES 1979 *Journal of Sound and Vibration* **65**, 275–296. A magnetoelastic strange attractor.
14. P. J. HOLMES and J. E. MARSDEN 1981 *Archive for Rational Mechanics and Analysis* **76**, 135–166. A partial differential equation with infinitely many periodic orbits: chaotic oscillations of a forced beam.
15. B. D. GREENSPAN and P. J. HOLMES 1981 in *Nonlinear Dynamics and Turbulence* (editors G. Barenblatt, G. Iooss and D. D. Joseph), London: Pitman Press. Homoclinic orbits, subharmonics and global bifurcations in forced oscillations.
16. C. S. HSU 1977 *Advances in Applied Mechanics* **17**, 245–301. On nonlinear parametric excitation problems.
17. J. BERNOUSSOU 1977 *Point Mapping Stability*, New York: Pergamon Press.
18. G. SCHMIDT 1980 *Physical Review* **A22**, 2849–2854. Stochasticity and fixed point transitions.
19. S. SMALE 1963 in *Differential and Combinational Topology* (editor S. S. Cairns). Princeton University Press. Diffeomorphisms with many periodic points.
20. N. LEVINSON 1949 *Annals of Mathematics* **50**, 127–153. A second order differential equation with singular solutions.
21. M. LEVI 1981 *Memoirs of the American Mathematical Society* **244**. Qualitative analysis of the periodically forced relaxation oscillations.
22. J. MOSER 1973 *Stable and Random Motions in Dynamical Systems*. Princeton University Press.
23. Z. NITECKI 1971 *Differentiable Dynamics*. M.I.T. Press.
24. S. NEWHOUSE 1980 in *Dynamical Systems, CIME Lectures, Bressanone, Italy, June* 1978, *Progress in Mathematics*, No. 8. Boston: Birkhauser-Boston Inc. Lectures on dynamical systems.
25. P. STEFAN 1977 *Communications in Mathematical Physics* **54**, 237–248. A theorem of Sarkovskii on the existence of periodic orbits of continuous endomorphisms of the real line.
26. J. GUCKENHEIMER 1977 *Inventiones Mathematical* **39**, 165–178. Bifurcations of maps of the interval.
27. P. COLLET, J. P. ECKMANN and O. E. LANFORD 1980 *Communications in Mathematical Physics* **76**, 211–254. Universal properties of maps on an interval.
28. P. COLLET and J. P. ECKMANN 1980 *Iterated Maps on the Interval as Dynamical Systems, Progress in Physics*, No. 1. Boston: Birkhauser-Boston, Inc.
29. S. NEWHOUSE 1979 *Publications Mathématiques of the Institut des Hautes Etudes Scientifiques* **50**, 101–151. The abundance of wild hyperbolic sets and non-smooth stable sets for diffeomorphisms.
30. N. K. GAVRILOV and L. P. SILNIKOV 1972–73 *Mathematics USSR Sbornik* **88**, 467–485 and **90**, 139–156. On three dimensional dynamical systems close to systems with a structurally unstable homoclinic curve, I and II.
31. M. HÉNON 1976 *Communications in Mathematical Physics* **50**, 69–77. A two dimensional mapping with a strange attractor.
32. C. S. HSU, H. C. YEE and W. H. CHENG 1977 *American Society of Mechanical Engineers, Journal of Applied Mechanics* **44**, 147–153. Determination of global regions of asymptotic stability for difference dynamical systems.
33. M. A. LIEBERMAN 1981 Personal communication.
34. R. V. JENSEN and C. R. OBERMAN 1981 *Princeton Plasma Physics Laboratory Report PPPL-1764*. Calculation of the statistical properties of strange attractors.
35. R. V. JENSEN and C. R. OBERMAN 1981 *Princeton Plasma Physics Laboratory Report PPPL-1780*. Statistical properties of chaotic dynamical systems which exhibit strange attractors.